Published in final edited form as:
J Bone Miner Res. 2012 October ; 27(10): 2097–2107. doi:10.1002/jbmr.1662.

Villin Promoter-Mediated Transgenic Expression of TRPV6 Increases Intestinal Calcium Absorption in Wild-type and VDR Knockout Mice

Min Cui, PhD[1,#], **Qiang Li, PhD**[1], **Robert Johnson, DVM**[2], and **James C. Fleet, PhD**[1]

[1] Department of Nutrition Science, Purdue University, West Lafayette, Indiana

[2] Department of Comparative Pathobiology, Purdue University, West Lafayette, Indiana

Abstract

Transient receptor potential cation channel, subfamily V, member 6 (TRPV6) is an apical membrane calcium (Ca) channel in the small intestine proposed to be essential for vitamin D regulated intestinal Ca absorption. Recent studies have challenged the proposed role for TRPV6 in Ca absorption. We directly tested intestinal TRPV6 function in Ca and bone metabolism in wild-type (WT) and vitamin D receptor knockout (VDRKO) mice. Transgenic mice (TG) were made with intestinal epithelium-specific expression of a 3X flag-tagged human TRPV6 protein. TG and VDRKO mice were crossed to make TG-VDRKO mice. Ca and bone metabolism was examined in WT, TG, VDRKO, and TG-VDRKO mice. TG mice developed hypercalcemia and soft tissue calcification on a chow diet. In TG mice fed a 0.25% Ca diet, Ca absorption was >3 fold higher and femur bone mineral density (BMD) was 26% higher than WT. Renal CYP27B1 mRNA and intestinal expression of the natural mouse TRPV6 gene were reduced to <10% of WT but small intestine calbindin-D_{9k} expression was elevated >15X in TG mice. TG-VDRKO mice had high Ca absorption that prevented the low serum Ca, high renal CYP27B1 mRNA, and low BMD and abnormal bone microarchitecture seen in VDRKO mice. In addition, small intestinal calbindin D_{9K} mRNA and protein levels were elevated in TG-VDRKO. Transgenic TRPV6 expression in intestine is sufficient to increase Ca absorption and bone density, even in VDRKO mice. VDR independent up-regulation of intestinal calbindin D_{9k} in TG-VDRKO suggests this protein may buffer intracellular Ca during Ca absorption.

Keywords

TRPV6; calbindin D_{9k}; vitamin D; intestine; absorption

Correspondence and reprint requests: James C Fleet, PhD Department of Nutrition Science Purdue University 700 West State Street West Lafayette, Indiana 47907-2059 fleet@purdue.edu (O) 1-765-494-0302 (F) 1-765-494-0906.
[#]**Current address:** Min Cui, PhD, Carnegie Institution of Washington, Department of Embryology, 3520 San Martin Drive, Baltimore, Maryland 21218, USA

Disclosures: All authors state that they have no conflicts of interest.

Author roles:
JCF conceived the research hypothesis, obtained funding, supervised the research conducted to test the hypothesis, and wrote the final version of the manuscript; MC created the transgene construct, completed the animal work described, conducted the analysis of most of the studies, compiled and analyzed the data, and wrote the first complete draft of the manuscript, QL conducted analysis of tissue mRNA and protein levels in the TG-VDRKO mouse study, summarized and analyzed that data, and provided comments on the manuscript, RJ, conducted the histological examination of tissues from transgenic mice and provided comments on the manuscript.

Introduction

Calcium (Ca) is essential for the integrity of bone and it is necessary for physiological functions such as muscle contraction, neurotransmission, and secretion (1). Whole body Ca metabolism is controlled by a three tissue axis of intestine, kidney, and bone to maintain extracellular Ca concentration within a narrow range. Vitamin D-regulated intestinal Ca absorption is a key player in overall Ca homeostasis (2), and it occurs through both saturable, transcellular and non-saturable, paracellular diffusion pathways (3). While several models for transcellular intestinal Ca transport have been proposed, the most studied model is the facilitated diffusion model where transport occurs in three steps: entry across the apical brush border membrane through the Ca channel Transient Receptor Potential cation channel, subfamily V, member 6 (TRPV6); intracellular diffusion/transportation to the basolateral side of the cell mediated by calbindin D_{9k}, and extrusion across the basolateral membrane by plasma membrane Ca ATPase 1b (PMCA1b) (3).

Several observations are consistent with the hypothesis that TRPV6 mediates apical membrane entry of calcium into enterocytes: TRPV6 is abundantly expressed in duodenum, its expression level is up-regulated by low dietary Ca intake and by 1,25-dihydroxyvitamin D_3 (1,25$(OH)_2$D) injection, and increased TRPV6 mRNA levels precede the elevation of Ca absorption after 1,25$(OH)_2$D injections (4). In addition, TRPV6 mRNA levels are reduced by 95% in vitamin D receptor (VDR) knockout mice and this is accompanied by a 70% reduction in intestinal Ca absorption efficiency (5;6). However, several recent studies in TRPV6 knockout mice have challenged the central role proposed for TRPV6 in intestinal Ca absorption. For example, in contrast to VDR knockout mice who have severe hypocalcemia and rickets caused by very low intestinal Ca absorption (2;5), TRPV6 knockout mice have normal serum Ca level and they respond to dietary Ca restriction and 1,25$(OH)_2$D injections by increasing intestinal Ca absorption efficiency (7-9). However, while these studies demonstrate that vitamin D mediated intestinal Ca absorption can occur in the absence of TRPV6, a direct test of whether TRPV6 can mediate intestinal Ca absorption has not yet been conducted. To examine the *in vivo* role of TRPV6 in intestinal Ca transport, we created transgenic mice expressing human TRPV6 in intestinal epithelial cells. We then examined the impact of transgenic TRPV6 expression on Ca and bone metabolism.

Materials and Methods

Animals

All animal experiments were approved by the Purdue Animal Care and Use Committee. Mice were exposed to a 12-h light/12-h dark cycle, and food and water were given *ad libitum*.

Generation of 3XFlag-hTRPV6 Expressing Transgenic Mice

Trangenic mice expressing human TRPV6 under control of the villin promoter/enhancer were generated using the vector shown in Figure 2A. The transgene was constructed in the pUC12.4-kb-villin plasmid (10). The human TRPV6 fragment (hTRPV6) from the plasmid pBS II SK-hTRPV6 was subcloned into the pN3XFlag plasmid (11) to generate the pN3XFlag-hTRPV6 vector that encodes hTRPV6 with three Flag sequences on the N-terminal end of the protein. The 3XFlag-hTRPV6 fragment was subcloned into the Xho I and Age I site of the pUC12.4-kb-villin plasmid to generate the pUC12.4k-villin-3XFlag-hTRPV6 plasmid (Figure 2A). After digestion with Pme I, the 16-kb transgene was used to create TRPV6 transgenic mice (TG) at the Purdue University Transgenic Mouse Core Facility using standard pronuclei injection methods. Oocytes were from C57BL/6N mice and they were implanted into recipient females on the C57BL/6J genetic background. The

transgene was detected in tail genomic DNA by conventional PCR and the transgene copy number was determined using real-time PCR. Transgenic mice were maintained by breeding males to C57BL/6J females. Analysis of the transgene distribution was conducted after 2-3 crosses onto the C57BL/6J background. Characterization of the transgenic mouse was conducted after 5-8 crosses onto the C57BL/6J background. Characterization of the a cross between the transgenic mouse and the VDR knockout mouse (on the C57BL/6J background) was conducted after more than 10 crosses to the C57BL/6J background.

Caco-2 cell culture and experiments

Cells were grown using medium and conditions that we have described previously (12). The ability of this vector to drive expression of hTRPV6 labeled on the N-terminal end with 3 Flag sequences was tested by transient transfection of Caco-2 cells. Proliferating cultures of Caco-2 cells were transiently transfected with the pN3XFlag-hTRPV6 expression vector using conditions we have described previously (12). Two days after transfection cell surface proteins were labeled by biotinylation and isolated using Avidin-bound agarose column (Pierce Cell Surface Protein Isolation Kit, Pierce Biotechnology, Rockford, IL). Whole cell extracts, flow-through from the columns, and material that bound to the columns were subjected to SDS-PAGE and TRPV6 was detected by immunoblotting using the methods described below.

Evaluation of the Phenotype of TRPV6 Transgenic and TRPV6 Transgenic-VDR Knockout mice

Female TG and WT mice were fed either a standard commercial chow diet (0.72% Ca) or an AIN93G based diet (13) containing 0.25% Ca and 200 IU vitamin D (Research Diets, New Brunswick, NJ) from weaning until 8 wks of age. VDR knockout mice (VDRKO) were crossed to TRPV6 transgenic mice (TG) to make TG-VDRKO mice using traditional breeding. All mice used were on the C57BL/6J genetic background. Age and gender matched WT, VDRKO, TG, TG-VDRKO mice were obtained and fed AIN93G diets containing 0.5% Ca diet and 1000 IU vitamin D_3/kg diet (Research Diets) from weaning to 10 wks of age. At the end of the feeding periods, mice were fasted overnight (12 h). Ca absorption was measured as appearance of ^{45}Ca in serum 10 minutes after oral gavage as described previously (6). Blood samples were obtained at 10 min after oral gavage, and serum (10 μl) was analyzed by liquid scintillation counting.

Serum was analyzed for Ca (QuantiChrom assay, BioAssay Systems, Hayward, CA) and $1,25(OH)_2D$ levels (ImmunoDiagnostic Systems, Fountain Hills, AZ). A spot urine sample was taken and analyzed for Ca and creatinine (QuantiChrom Ca and Creatinine kits). Mucosa scrapings from intestine segments, including duodenum, jejunum, ileum, proximal colon, distal colon, and kidneys were harvested for analysis of gene expression. Femora were harvested for the assessment of bone mineral density (BMD) by DEXA and for microarchitecture using micro-Computed Tomography (μCT) and histomorphometry (2).

Conventional and Real-time PCR

The transgene was detected in tail genomic DNA by conventional PCR and the transgene copy number was determined using real-time PCR using the primers P1 and P2 (primer P1: $^{5'}$ CTCGAGCTAGACCATGGACTACAAA $^{3'}$, primer P2: $^{5'}$TGGCAGCTAGAAGGAGAGGA$^{3'}$; Tm, 55.8°**C**; PCR product, 248 bp, Figure 2A) as described previously (14). Total RNA was isolated and reverse-transcribed into cDNA as previously described (2). Transgene mRNA was measured by conventional PCR or real-time PCR using primers P2 and P3 (P3: $^{5'}$TGGCTGCCTCTTCCAGACAG$^{3'}$; Tm, 55.8°**C**; PCR product, 290 bp). Primers TRPV6 #1 and TRPV6 #2 (12) recognize regions common to the human and mouse TRPV6 transcript and were used to measure total TRPV6 mRNA level.

Primers mTRPV6 #1 and mTRPV6 #2 (#1: $^{5'}$AAGCTACCTCGTTGCCTGTG$^{3'}$, #2: $^{5'}$AGTAGAGGCCATCTTGTTGC$^{3'}$; Tm, 57.0 °**C**; PCR product, 157 bp) were used to measure mouse TRPV6 mRNA level. Primers mRPLP0 #1 and mRPLP0 #2 (#1: $^{5'}$AGAAACTGCTGCCTCACATCC$^{3'}$, #2: $^{5'}$CAATGGTGCCTCTGGAGATT$^{3'}$; Tm, 59.0°**C**; PCR product, 229 bp) were used to measure the mRNA level for the housekeeping gene, ribosomal protein, large, P0 (RPLP0). Primers and conditions for analysis of CYP24, CYP27B1, calbindin D_{9k}, TRPV5, VDR and calbindin D_{28k} mRNA level have been reported previously by our group (2;15).

Immunoblotting

In some studies cell and tissue extracts were subjected to differential centrifugation as described by Kessler et al. (16). Mucosa scrapings or cell pellets were homogenized in ice-cold lysis buffer (50 mmol/L mannitol, 2 mmol/L Tris, pH 7.2, 50 μg/ml benzamidine) with complete proteinase inhibitor cocktail (Roche Applied Science, Indianapolis, IN), 1 mmol/L PMSF and calcium added to 10 nmol/L. After clearing whole cells from the homogenate (3000 × g, 10 min, 4°C) a primary pellet containing cell membranes was prepared (P1, 30,000 × g, 20 min, 4°C). This pellet was resuspended in lysis buffer and centrifuged again to isolate a pellet containing brush border membranes (BBM)(P2, 43,000 × g, 30 min, 4°C). The BBM pellet was resuspended in the lysis buffer and used for Western blot analysis. For other analyses, mucosa scrapings were homogenized in ice-cold modified lysis buffer (300 mmol/L mannitol, 10 mmol/L Tris, pH 7.2, 50 μg/ml benzamidine) with complete proteinase inhibitor cocktail (Roche Applied Science, Indianapolis, IN) and 1 mmol/L PMSF to make whole cell extracts (WCE). The whole cell extract was centrifuged at 16,300 × g for 30 minutes at 4°C and the supernatants were used for immunoblotting.

For the TRPV6 western blot, 80 μg of BBM protein or 30 μg of WCE protein were separated on 7.5% Tris-glycine polyacrylamide gels and transferred to PVDF membranes using standard Western blot procedures. Rabbit anti-TRPV6 primary antibody (1:2000 dilutions, Alomone Labs Ltd, Israel) and HRP conjugated goat anti rabbit secondary antibody (1:5000 dilutions, Zymed, Carlsbad, CA) were used. For calbindin D_{9k}, 60 μg of whole cell extracts from intestine segments and 50 ng calbindin D_{9k} standard (Sigma-Aldrich, St. Louis, MO) were separated on 16.5% Tris-HCl polyacrylamide gels. Rabbit anti-calbindin D_{9k} primary antibody (1:2000 dilutions, Swant, Switzerland) was used for detection. Membranes were stripped and reprobed with β-actin antibody as described previously (12). Specific antibody binding to blots was determined by chemiluminescent detection (SuperSignal West Pico Chemiluminescent substrate, Pierce, Rockford, IL).

Bone Analysis

Femora were harvested and fixed in 10% neutral buffered formalin for 7 days and stored in 75% ethanol at 4°**C** until the samples were processed. Fixed femora were scanned using a PIXImus densitometer (Lunar; GE-Healthcare, Madison, WI) to determine bone mineral content (BMC, in grams) and bone mineral density (BMD, in g/cm^2) as described previously (2). For μCT mouse femora were scanned using a μCT 40 desktop scanner (Scanco Medical Ag, Bruttisellen, Switzerland) at a resolution of 6 μm^3, 55 kVp energy, 145 μA intensity, and a 300 ms integration time. Data are reported using nomenclature described previously (17). Trabecular bone was assessed by scanning and reconstructing a 1.5 mm region (150 slices) 0.3 mm proximal to the apex of the distal condyle and reported as volume/total volume (BV/TV, %), trabecular number (Tb.N, 1/mm), trabecular spacing (Tb.Sp, mm), and trabecular thickness (Tb.Th, mm). Cortical bone at the femoral midshaft was assessed by evaluating a 0.25 mm region (40 slices) at 50% total femur length and are reported as cortical area to total area (Ct.Ar/Tt.Ar, %) and cortical thickness (Cort.Th, mm). For histology, calcified femora were processed by the Centre for Bone and Periodontal Research

at McGill University (Montreal, Canada) as described previously (2). Sections were examined for mineralization using the Von Kossa staining procedure and counterstained with toluidine blue.

Statistical Analysis

All data are presented as the mean ± SEM. Studies were analyzed by ANOVA followed by Fisher's protected LSD. If predicted versus residual plots showed that the data were not normally distributed, data were log transformed prior to analysis. P-Values less than 0.05 were considered statistically significant.

Results

Assessment of intestinal TRPV6 expression in mice and transfected Caco-2 cells

We initially examined the expression of mouse TRPV6 protein in mouse intestine. TRPV6 is a 75 kd protein that can be glycosylated so it appears in the range of 75-100 kd on SDS PAGE (18). TRPV6 protein in WT mice was observed in brush border membrane preparations in all intestinal segments where mRNA is present. In the brush border membrane of duodenum the protein is predominantly the high molecular weight, glycosylated form (see Figure 1A). In addition, the size of the TRPV6 protein band was higher in duodenum than the other small intestinal segments (Figure 1B) suggesting TRPV6 in jejunum and ileum is not glycosylated. Consistent with the 95% reduction in TRPV6 mRNA level we have previously reported in VDR KO mice (19), TRPV6 protein was not detected in the intestinal scrapings of VDR KO mice (Figure 1B). We next examined whether the 3X Flag-tagged hTRPV6 transgene we created would be expressed, localized, and glycosylated appropriately by transiently expressing the protein in the human intestinal cell line Caco-2. Figure 1C shows that two hTRPV6 bands were expressed in transfected Caco-2 cells; the higher molecular weight protein is a cell surface protein that can be biotinylated and isolated. This confirmed that our transgene was likely to be expressed at the apical membrane surface when expressed in mice.

Characterization of TRPV6 Transgenic mice

Four transgenic founders were obtained. Of these, two did not transmit the transgene to their offspring and only one of the others expressed both transgene mRNA and protein in the intestine. The line expressing both transgene mRNA and protein was studied further. Consistent with the reported expression of the villin promoter (10), transgene mRNA was detectable at high levels throughout the intestine and at low levels in the kidney. All other tissues were transgene negative (Figure 2B). Transgene mRNA was highest in duodenum and jejunum; colonic transgene mRNA levels were elevated but were 90% lower than levels seen in the duodenum (Figure 2C). While renal transgene mRNA was elevated relative to wild-type levels (by 300-fold, data not shown), the total TRPV6 levels in the kidneys of transgenic mice were still only 1% of the level found in their duodenum. Transgene expression increased TRPV6 protein level throughout the intestine, with the highest expression levels found in the small intestine (Figure 2D).

TG mice were initially fed a standard, high Ca chow diet. However, on this diet the growth of TG mice was poor. Necropsy and histological analysis of TG mice fed the chow diet revealed soft tissue calcification in kidney, heart, blood vessels, lung and stomach (see Supplemental Figure 1). Serum and urine Ca levels were elevated in chow-fed 3 mo-old TG and WT mice (serum: WT = 10.8±0.7 mg/dl, TG = 14.0±1.4 mg/dl; urine: WT = 17.2±4.1 mg/dl, TG = 25.7±3.5 mg/dl, n=3/group). Subsequent studies were conducted in mice fed semi-purified diets with reduced Ca content (0.25%). This diet normalized serum Ca (WT 0.25% Ca diet = 9.11±1.31 mg/dl, TG 0.25% Ca = 10.83±0.42 mg/dl, Figure 3A) and body

weight at 2 mo (WT = 16.1±0.5 g, TG 15.6±0.8 g). However, even on the low Ca diet, transmission of the transgene to offspring was poor. No TG pups were generated when female TG mice were paired with WT male mice. When male TG mice were bred with female WT mice, transgene transmission rate was less than 25% (see Supplemental Table 1).

Ca Absorption and Bone Phenotype of Transgenic Mice

Ca absorption in 8-wk-old female fed the 0.25% Ca diet was 3-fold higher than WT mice (Figure 3B). Consistent with other reports (20) (21) hyperabsorption of Ca accounts for the elevated urinary Ca levels we observed in TG mice. In addition, the elevation of Ca absorption caused by transgene TRPV6 expression in intestine, and perhaps even increased renal transgene TRPV6 expression in kidney, account for elevated serum Ca levels in TG mice (Figure 3A). Femur length was not different between TG and WT mice (data not shown) but femur BMD in TG mice was higher than WT by 28% (Figure 3C). Femoral architecture was analyzed using μCT scanning of trabecular (distal) and cortical (midshaft) sites (Table 1). Like total BMD, cortical area fraction (Ct.Ar/Tt.Ar, +23%) and cortical thickness (Ct.Th, +26%) were significantly increased in TG mice. At the distal femur, trabecular BV/TV (+802%), trabecular number (Tb.N, +78%), and trabecular thickness (Tb.Th, +66%) were all significantly higher, while trabecular spacing (Tb.Sp) was significantly lower (-48%), in TG than WT. Consistent with the μCT data, Von Kossa staining also showed more and larger trabeculae in distal femur (Figure 3D).

Renal and Intestinal Gene Expression in Transgenic Mice

Renal CYP27B1 mRNA was 98% lower and renal CYP24 mRNA was elevated 17-fold in TG (Figure 4A) leading to low serum levels of $1,25(OH)_2$ D (reduced by 56%). Increased serum Ca and reduced serum PTH levels (46% lower) (Figure 5B) likely explain the suppression of renal CYP27B1 and low serum $1,25(OH)_2$ D levels. The reduction of $1,25(OH)_2$ D in TG mice caused the loss of mRNA levels for vitamin D regulated genes in the intestine; i.e. reduced expression of CYP24 mRNA (data not shown) and the natural mouse TRPV6 mRNA (11% of WT in duodenum, 3.6% in jejunum, 0.28% in proximal colon and 6.5% in distal colon, Figure 4B). In contrast, calbindin D_{9k} gene expression was strongly up-regulated in duodenum and jejunum of TG mice, but not in the colon (Figure 4C). Renal TRPV5 and calbindin D_{28k} expression were not changed. VDR mRNA level was not altered in any intestinal segment or in kidney of TG mice.

Effects of TRPV6 Transgene Expression on Phenotype of VDR Knockout Mice

When fed the 0.5% Ca AIN93G diet, VDRKO mice are growth arrested (-14%) and have hypocalcemia (-26%, Figure 5A), elevated serum $1,25(OH)_2$ D (+28.6-fold, Figure 5B), elevated serum PTH (+20.5-fold, Figure 5B), and reduced bone mass (e.g. midshaft cortical bone thickness -58%, Table 2) relative to WT mice. In TG-VDRKO mice, body weight was improved but not normalized (WT = 21.8±1.1 g, VDRKO = 18.8±0.9 g, TG = 20.5±0.7 g, TG-VDRKO = 19.2±1.1 g, n=6-10/group). In contrast, the negative effects of VDR deletion on femora in VDRKO were reversed in TG-VDRKO and exceeded WT values (Table 2). At the distal femur BV/TV (+3.7-fold), Tb.N (+91%), and Tb.Th (+22%) were elevated and Tb.Sp (-49%) decreased in TG-VDRKO mice compared to WT mice. At the midshaft femur, Ct.Ar/Tt.Ar was normalized in TG-VDRKO and Ct.Th was increased in TG-VDRKO to 19% higher than WT values.

The low serum Ca level seen in VDRKO mice was eliminated in TG-VDRKO but was elevated relative to WT mice (+40%, Figure 5A) while the elevated serum $1,25(OH)_2$ D and PTH levels seen in VDRKO mice were reduced in TG-VDRKO to below values normally seen in WT mice (Figure 5B). In VDRKO mice renal CYP27B1 expression is up-regulated 620-fold and renal CYP24 mRNA was completely suppressed (Figure 5C). Consistent with

the increased serum Ca levels observed in TG-VDRKO mice, renal CYP27B1 mRNA was normalized and CYP24 mRNA levels were reduced in TG-VDRKO mice. Urinary Ca level was 109% higher in VDRKO (p=0.076), 8.9-fold higher in TG mice, and 22-fold higher in TG-VDRKO compared to WT mice (Figure 5D).

Intestinal Ca absorption in mice fed the 0.5% Ca diet was 53% lower in VDRKO and 6.2±1.0 fold higher in TG mice compared to WT mice (Figure 6A). The high Ca absorption level from TG mice was maintained in TG-VDRKO mice (5.3±0.74 fold above WT). The phenotype of elevated intestinal Ca absorption from TG mice, coupled with elevated urinary Ca from VDRKO mice (2) explains why urinary Ca was increased to 22-fold over WT levels (and 2.5-fold higher than TG) in TG-VDRKO. Intestinal calbindin D_{9k} mRNA levels were significantly reduced in VDRKO (>50% lower in all segments, Figure 6B). Despite the absence of intestinal VDR, the elevated calbindin D_{9k} mRNA in the TG intestine was also present in TG-VDRKO mice, i.e. strongly up-regulated in duodenum and jejunum (17- and 21-fold respectively, compared to WT duodenum). Western blot analyses confirmed that calbindin D_{9k} protein levels were strongly elevated in the duodenum of both TG and TG-VDRKO mice (Figure 6C).

Discussion

Dysregulation of intestinal Ca absorption occurs with aging (22;23) and following the menopause (24-26) leading to low fractional Ca absorption that increases hip fracture risk in women with low dietary Ca intake (27). In addition, intestinal Ca hyperabsorption can cause hypercalciuria leading to the formation of kidney stones in rats (20) and humans (21). Understanding the mechanisms controlling active intestinal Ca absorption will aid the search for preventative or therapeutic approaches to these diseases.

Four models have been proposed to explain the mechanism for intestinal Ca absorption: vesicular trafficking, transcaltachia, regulated paracellular transport, and the most studied of these mechanisms, the facilitated diffusion model (see (3) for a detailed discussion of these mechanisms). In the facilitated diffusion model, basal and vitamin D-dependent uptake of Ca across the brush border membrane into the enterocyte is mediated by TRPV6 (28). Ca uptake has been proposed as the rate limiting step for intestinal Ca absorption by some (29;30) but not others (31;32). However, our current report is the first direct demonstration that TRPV6 is a functional apical membrane Ca transporter in the mammalian intestine and that it can mediate intestinal Ca absorption. Prior to our studies others had reported relationships that were consistent with a role for TRPV6 in intestinal Ca absorption but were based on TRPV6 mRNA levels. For example, the TRPV6 gene is a direct vitamin D target gene (12;33;34) so TRPV6 mRNA level is reduced by more than 90% in the duodenum of VDRKO mice and this coincides with reduced intestinal Ca absorption. TRPV6 gene expression is strongly up-regulated by $1,25(OH)_2$ D in cultured intestinal cells (12;35) and in the duodenum of mice (4;34) and humans (36); because of this there is a positive correlation between TRPV6 mRNA levels and intestinal Ca absorption when dietary Ca is varied (4).

Finally, induction of TRPV6 mRNA precedes the increase in duodenal Ca absorption that occurs following a single $1,25(OH)_2$ D injection (4). Based on these relationships and on the proposed role for TRPV6 in the facilitated diffusion model, researchers hypothesized that deletion of the TRPV6 gene would result in a phenotype similar to the VDR knockout mouse, i.e. impaired Ca absorption (4;6), hypocalcemia, and osteomalacia (37;38). However, three reports show that intestinal Ca absorption is still present and that it increases in response to $1,25(OH)_2$ D injection or dietary Ca restriction in TRPV6 knockout mice (7-9). These data suggest that the presence of TRPV6 is not an absolute requirement for

vitamin D regulated intestinal Ca absorption. However, these studies did not directly test TRPV6 function as an intestinal Ca transporter nor did they eliminate the possibility that there are other apical membrane Ca transporters that can compensate for the loss of TRPV6 in the knockout mouse. Our approach directly demonstrates that TRPV6 can function as an apical membrane Ca transporter by showing that intestinal Ca absorption is elevated more than 300% in mice with intestine-specific transgenic expression of TRPV6. This is sufficient to overcome the defect of abnormal Ca absorption in VDRKO mice and to completely prevent the adverse phenotypes associated with the loss of VDR. We previously demonstrated that the major phenotypes of VDRKO mice could be prevented by intestine-specific transgenic expression of VDR (2); this is presumably because all vitamin D-dependent intestinal events were restored. We extend that observation by showing that the primary defect in VDRKO mouse leading to hypocalcemia and osteomalacia is the inability to move Ca into the enterocyte. Our data show that once the apical barrier has been crossed (i.e. TRPV6 permits apical membrane entry of Ca), all other components of the intestinal Ca absorption system are sufficient to permit transcellular movement in VDRKO mice. Our work does not explain how vitamin D regulated Ca absorption can occur in mice lacking TRPV6. Future studies will be needed to identify the alternative Ca entry pathways that function in TRPV6 KO mice.

Our results also address the role that calbindin D_{9k} may play during intestinal Ca absorption. Calbindin D_{9k} was originally proposed to facilitate transcellular movement of Ca from the apical Ca channel to the basolateral Ca pump during intestinal absorption (31). Its protein levels positively correlate to Ca absorption over a wide range of biological conditions including vitamin D deficiency or VDR deletion (31). Under these conditions calbindin D_{9k} expression correlates with TRPV6 mRNA expression (5;6;39) and this is consistent with the belief that both genes are directly regulated by $1,25(OH)_2$ D through the VDR. Disruption of Ca binding to calbindin D_{9k} with theophylline reduces intestinal Ca absorption in rats (40) and this suggests that calbindin D_{9k} is necessary for transcellular Ca absorption. In contrast, several studies have shown that calbindin D_{9k} is not essential for intestinal Ca absorption. For example, after $1,25(OH)_2$ D treatment intestinal calbindin protein levels rise but only after increases in Ca absorption occur (4;41). In addition, intestinal Ca absorption can be low even when calbindin protein levels are elevated (5;42). Studies in calbindin D_{9k} knockout mice confirm that this protein is not essential for basal or vitamin D regulated intestinal Ca absorption (8;43;44).

We expected that the suppression of $1,25(OH)_2$ D production caused by elevated Ca absorption in TRPV6 transgenic mice would reduce expression of the calbindin D_{9k} gene – much like it did for intestinal CYP24 and the natural mouse TRPV6 gene. Instead, we found that calbindin D_{9k} was elevated in TRPV6 TG and TG-VDRKO mice. We believe that this supports a buffer function for calbindin D_{9k}, i.e. induction is a response to increased intracellular Ca during Ca absorption and that these changes are independent serum $1,25(OH)_2$ D. Calbindin D_{28k} was previously shown to be a Ca buffer within mammalian nervous tissue (45;46) and its expression can suppress apoptosis in lymphocytes and osteoblasts (47;48). In addition, calbindin D_{9k} can buffer ionomycin-induced rises in intracellular Ca in isolated pig enterocytes (49). However, further tests of the buffer hypothesis are necessary to determine whether the large increase in calbindin D_{9k} in TRPV6 TG mice protects the enterocyte from negative consequences of excess intracellular Ca like promoting apoptosis of differentiated cells or proliferation of cells in the intestinal crypt. There is also another role for calbindin D_{9k} that may be relevant to our data. Previously Lambers et al. (50) showed that in the rabbit connecting tubule/distal convoluted tubule, calbindin D_{28k} directly associates with the renal apical membrane Ca channel TRPV5. This association permits calbindin D_{28k} to act as a dynamic, local Ca buffer that prevents Ca-mediated inactivation of TRPV5. While a similar interaction has been proposed between

TRPV6 and calbindin D_{9k} this local role has not yet been demonstrated. Future studies with our model may permit demonstration of this interaction and testing of this role.

Our data from TG-VDRKO mice also show that intestinal calbindin D_{9k} and renal CYP24 mRNA can be regulated by means other than 1,25$(OH)_2$ D. The CYP24 gene is the most vitamin D-responsive target gene that has been identified and previous cell-based studies show that expression of the gene does not occur in the absence of the hormone (12;51;52). Since up-regulation of renal CYP24 mRNA due to TRPV6 transgene expression occurs even in VDRKO mice (i.e. is vitamin D independent), we propose this is due to elevated serum or urinary Ca levels and perhaps signaling through the Ca sensing receptor. Consistent with this, Anderson et al. (53) reported that renal CYP24 mRNA was increased 5-fold in rats fed a 1 % Ca diet compared to those fed a 0.4% Ca diet. Others have shown that extracellular Ca regulates renal CYP27B1 mRNA (54), keratinocyte CYP1A1 mRNA (55), and hepatic 25 hydroxylase activity (56). Future studies are necessary to determine whether the same is true for the CYP24 gene. Duodenal calbindin D_{9k} levels are increased by 1,25$(OH)_2$ D injections (4;57) and others have identified putative VDREs in the calbindin D_{9k} promoter (58;59). However, we and others have found that calbindin D_{9k} is strongly up-regulated during enterocyte differentiation by the transcription factors HNF-1 and Cdx-2 but that the VDREs identified by others are not functional (60-62). We do not know what regulators account for the increase of calbindin D_{9k} in TRVP6 TG mice but we propose that increased intracellular Ca flux resulting from elevated TRPV6 expression increases calbindin D_{9k} gene expression, increases mRNA stability, or promotes development of more differentiated enterocytes (which express high levels of calbindin D_{9k}). Related to this, we found more modest increases in calbindin D_{9k} mRNA in the colon even though TRPV6 protein levels were also elevated in these tissues within TRPV6 TG mice. We hypothesize that the lower expression of calbindin D_{9k} in the colon is due to the fact that less Ca is entering the colonocyte through TRPV6. This could be due to the lower level of TRPV6 protein we observed in the colon of transgenic mice or because Ca is not available for transport into the enterocytes due to reduced intestinal solubility of Ca in the alkaline environment of the large bowel (63).

In summary, we have demonstrated that the apical membrane Ca transporter TRPV6 is functional and can be used to increase transcellular intestinal Ca absorption. Our data show that by overcoming the barrier of low apical membrane Ca uptake caused by VDR gene deletion, TRPV6 can prevent the formation of hypocalcemia and osteomalicia seen in the VDRKO mouse. This demonstrates that apical membrane Ca movement is the primary defect in VDRKO mice. Finally, our data also suggest a role for calbindin D_{9k} as an intracellular buffer to prevent adverse cellular effects caused by elevated transcellular Ca flux.

Supplementary Material

Refer to Web version on PubMed Central for supplementary material.

Acknowledgments

The authors would like to thank the following: Purdue University: Ms. Rebecca Replogle, Ms. Marsha Desmet, Ms. Bernardine Frankel, Ms. Yan Li and Mr. Hector Ochoa for technical assistance with the animal studies; Dr. Debra Gumucio (University of Michigan) for the plasmid pUC12.4-kb-villin, Dr. Ji-Bin Peng (University of Alabama at Birmingham) for the plasmid pBS II SK-hTRPV6 and Dr. Jiguo Chen (Mississippi State University, MS) for the plasmid pN3XFlag.

Grant support: The work was supported by awards from the American Society of Bone and Mineral Research (BRIDGE06082) and the National Institutes of Health (DK054111) to J.C.F.

Abbreviations used in this paper

BMD	bone mineral density
Ca	calcium
CYP24	25-hydroxyvitamin D, 24-hydroxylase
CYP27B1	1α hydroxylase
SEM	standard error of the mean
TG	TRPV6 transgenic
TRPV5	Transient receptor potential cation channel, subfamily V, member 5
TRPV6	Transient receptor potential cation channel, subfamily V, member 6
VDR+/-	VDR heterozygous
VDRKO	vitamin D receptor knockout
WT	wild type
μCT	microcomputed tomography
1,25(OH)$_2$D	1,25-dihydroxyvitamin D_3

Reference List

1. Fleet, JC. Molecular Regulation of Calcium Metabolism.. In: Weaver, CM.; Heaney, RP., editors. Calcium in Human Health. Humana Press; Totowa, NJ: 2006. p. 163-190.
2. Xue Y, Fleet JC. Intestinal vitamin D receptor is required for normal calcium and bone metabolism in mice. Gastroenterology. 2009; 136:1317–2. [PubMed: 19254681]
3. Fleet JC, Schoch RD. Molecular mechanisms for regulation of intestinal calcium absorption by vitamin D and other factors. Crit Rev Clin Lab Sci. 2010; 47:181–195. [PubMed: 21182397]
4. Song Y, Peng X, Porta A, Takanaga H, Peng JB, Hediger MA, Fleet JC, Christakos S. Calcium transporter 1 and epithelial calcium channel messenger ribonucleic acid are differentially regulated by 1,25 dihydroxyvitamin D3 in the intestine and kidney of mice. Endocrinology. 2003; 144:3885–3894. [PubMed: 12933662]
5. Song Y, Kato S, Fleet JC. Vitamin D Receptor (VDR) Knockout Mice Reveal VDR- Independent Regulation of Intestinal Calcium Absorption and ECaC2 and Calbindin D9k mRNA. J Nutr. 2003; 133:374–380. [PubMed: 12566470]
6. Van Cromphaut SJ, Dewerchin M, Hoenderop JG, Stockmans I, Van Herck E, Kato S, Bindels RJ, Collen D, Carmeliet P, Bouillon R, Carmeliet G. Duodenal calcium absorption in vitamin D receptor-knockout mice: functional and molecular aspects. Proc Natl Acad Sci U S A. 2001; 98:13324–13329. [PubMed: 11687634]
7. Bianco SD, Peng JB, Takanaga H, Suzuki Y, Crescenzi A, Kos CH, Zhuang L, Freeman MR, Gouveia CH, Wu J, Luo H, Mauro T, Brown EM, Hediger MA. Marked disturbance of calcium homeostasis in mice with targeted disruption of the Trpv6 calcium channel gene. J Bone Miner Res. 2007; 22:274–285. [PubMed: 17129178]
8. Benn BS, Ajibade D, Porta A, Dhawan P, Hediger M, Peng JB, Jiang Y, Oh GT, Jeung EB, Lieben L, Bouillon R, Carmeliet G, Christakos S. Active intestinal calcium transport in the absence of transient receptor potential vanilloid type 6 and calbindin-D9k. Endocrinology. 2008; 149:3196–3205. [PubMed: 18325990]
9. Kutuzova GD, Sundersingh F, Vaughan J, Tadi BP, Ansay SE, Christakos S, DeLuca HF. TRPV6 is not required for 1alpha,25-dihydroxyvitamin D3-induced intestinal calcium absorption in vivo. Proc Natl Acad Sci U S A. 2008; 105:19655–19659. [PubMed: 19073913]
10. Madison BB, Dunbar L, Qiao XT, Braunstein K, Braunstein E, Gumucio DL. Cis elements of the villin gene control expression in restricted domains of the vertical (crypt) and horizontal

(duodenum, cecum) axes of the intestine. J Biol Chem. 2002; 277:33275–33283. [PubMed: 12065599]

11. Chen J. Serial analysis of binding elements for human transcription factors. Nat Protoc. 2006; 1:1481–1493. [PubMed: 17406439]
12. Cui M, Zhao Y, Hance KW, Shao A, Wood RJ, Fleet JC. Effects of MAPK signaling on 1,25-dihydroxyvitamin D-mediated CYP24 gene expression in the enterocyte-like cell line, Caco-2. J Cell Physiol. 2009; 219:132–142. [PubMed: 19097033]
13. Reeves PG, Rossow KL, Lindlauf J. Development and testing of the AIN-93 purified diets for rodents: results on growth, kidney calcification and bone mineralization in rats and mice. J Nutr. 1993; 123:1923–1931. [PubMed: 8229309]
14. Alexander G, Erwin K, Byers N, Deitech J, Heiman-Patterson T. Effect of transgene copy number on survival in the G93A mouse model of ALS. Neurology. 2004; 62:A36.
15. Song Y, Fleet JC. Intestinal Resistance to 1,25 Dihydroxyvitamin D in Mice Heterozygous for the Vitamin D Receptor Knockout Allele. Endocrinology. 2007; 148:1396–1402. [PubMed: 17110426]
16. Kessler M, Acuto O, Storelli C, Murer H, Muller M, Semenza G. A modified procedure for the rapid preparation of efficiently transporting vesicles from small intestinal brush border membranes. Their use in investigating some properties of D-glucose and choline transport systems. Biochim Biophys Acta. 1978; 506:136–154. [PubMed: 620021]
17. Bouxsein ML, Boyd SK, Christiansen BA, Guldberg RE, Jepsen KJ, M++ller R. Guidelines for assessment of bone microstructure in rodents using microΓÇôcomputed tomography. Journal of Bone and Mineral Research. 2010; 25:1468–1486. [PubMed: 20533309]
18. Lu P, Boros S, Chang Q, Bindels RJ, Hoenderop JG. The beta-glucuronidase klotho exclusively activates the epithelial Ca2+ channels TRPV5 and TRPV6. Nephrol Dial Transplant. 2008; 23:3397–3402. [PubMed: 18495742]
19. Song Y, Kato S, Fleet JC. Vitamin D Receptor (VDR) Knockout Mice Reveal VDR-Independent Regulation of Intestinal Calcium Absorption and ECaC2 and Calbindin D9k mRNA. J Nutr. 2003; 133:374–380. [PubMed: 12566470]
20. Favus MJ. Hypercalciuria: lessons from studies of genetic hypercalciuric rats. J Am Soc Nephrol. 1994; 5:S54–S58. [PubMed: 7873746]
21. Odvina CV, Poindexter JR, Peterson RD, Zerwekh JE, Pak CY. Intestinal hyperabsorption of calcium and low bone turnover in hypercalciuric postmenopausal osteoporosis. Urol Res. 2008; 36:233–239. [PubMed: 18633606]
22. Bullamore JR, Gallagher JC, Wilkinson R, Nordin BEC, Marshall DH. Effect of age on calcium absorption. Lancet. 1970; 2:535–537. [PubMed: 4195202]
23. Need AG, O'Loughlin PD, Morris HA, Horowitz M, Nordin BE. The effects of age and other variables on serum parathyroid hormone in postmenopausal women attending an osteoporosis center. J Clin Endocrinol Metab. 2004; 89:1646–1649. [PubMed: 15070925]
24. Gennari C, Agnusdei D, Nardi P, Civitelli R. Estrogen preserves a normal intestinal responsiveness to 1,25- dihydroxyvitamin D3 in oophorectomized women. J Clin Endocrinol Metab. 1990; 71:1288–1293. [PubMed: 2229286]
25. Heaney RP, Recker RR, Saville PD. Menopausal changes in calcium balance performance. J Lab Clin Med. 1978; 92:953–963. [PubMed: 739173]
26. Gallagher JC, Riggs BL, Eisman J, Hamstra A, Arnaud SB, DeLuca HF. Intestinal calcium absorption and serum vitamin D metabolites in normal subjects and osteoporotic patients: effect of age and dietary calcium. J Clin Invest. 1979; 64:729–736. [PubMed: 468987]
27. Ensrud KE, Duong T, Cauley JA, Heaney RP, Wolf RL, Harris E, Cummings SR. Low fractional calcium absorption increases the risk for hip fracture in women with low calcium intake. Study of Osteoporotic Fractures Research Group. Ann Intern Med. 2000; 132:345–353. [PubMed: 10691584]
28. Peng JB, Chen XZ, Berger UV, Vassilev PM, Tsukaguchi H, Brown EM, Hediger MA. Molecular cloning and characterization of a channel-like transporter mediated intestinal calcium absorption. J Biol Chem. 1999; 274:22739–22746. [PubMed: 10428857]

29. Nijenhuis T, Hoenderop JG, van der Kemp AW, Bindels RJ. Localization and regulation of the epithelial Ca2+ channel TRPV6 in the kidney. J Am Soc Nephrol. 2003; 14:2731–2740. [PubMed: 14569082]
30. Bouillon R, Van Cromphaut S, Carmeliet G. Intestinal calcium absorption: Molecular vitamin D mediated mechanisms. J Cell Biochem. 2003; 88:332–339. [PubMed: 12520535]
31. Bronner F, Pansu D, Stein WD. An analysis of intestinal calcium transport across the rat intestine. Am J Physiol. 1986; 250:G561–G569. [PubMed: 2939728]
32. Chandra S, Fullmer CS, Smith CA, Wasserman RH, Morrison GH. Ion microscopic imaging of calcium transport in the intestinal tissue of vitamin D-deficient and vitamin D-replete chickens: a 44Ca stable isotope study. Proc Natl Acad Sci U S A. 1990; 87:5715–5719. [PubMed: 2377608]
33. Meyer MB, Watanuki M, Kim S, Shevde NK, Pike JW. The human transient receptor potential vanilloid type 6 distal promoter contains multiple vitamin D receptor binding sites that mediate activation by 1,25-dihydroxyvitamin D3 in intestinal cells. Mol Endocrinol. 2006; 20:1447–1461. [PubMed: 16574738]
34. Meyer MB, Zella LA, Nerenz RD, Pike JW. Characterizing early events associated with the activation of target genes by 1,25-dihydroxyvitamin D3 in mouse kidney and intestine in vivo. J Biol Chem. 2007
35. Fleet JC, Eksir F, Hance KW, Wood RJ. Vitamin D-inducible calcium transport and gene expression in three Caco-2 cell lines. American Journal of Physiology-Gastrointestinal and Liver Physiology. 2002; 283:G618–G625. [PubMed: 12181175]
36. Walters JR, Balesaria S, Chavele KM, Taylor V, Berry JL, Khair U, Barley NF, van Heel DA, Field J, Hayat JO, Bhattacharjee A, Jeffery R, Poulsom R. Calcium channel TRPV6 expression in human duodenum: different relationships to the vitamin D system and aging in men and women. J Bone Miner Res. 2006; 21:1770–1777. [PubMed: 17002582]
37. Yoshizawa T, Handa Y, Uematsu Y, Takeda S, Sekine K, Yoshihara Y, Kawakami T, Arioka K, Sato H, Uchiyama Y, Masushige S, Fukamizu A, Matsumoto T, Kato S. Mice lacking the vitamin D receptor exhibit impaired bone formation, uterine hypoplasia and growth retardation after weaning. Nature Genetics. 1997; 16:391–396. [PubMed: 9241280]
38. Li YC, Pirro AE, Amling M, Delling G, Baron R, Bronson R, Demay MB. Targeted ablation of the vitamin D receptor: An animal model of vitamin D-dependent rickets type II with alopecia. Proc Natl Acad Sci USA. 1997; 94:9831–9835. [PubMed: 9275211]
39. Wasserman RH, Taylor AN. Vitamin D3-induced calcium-binding proteins in chick intestinal mucosa. Science. 1966; 252:791–793. [PubMed: 17797460]
40. Pansu D, Bellaton C, Roche C, Bronner F. Theophylline inhibits active Ca transport in rat intestine by inhibiting Ca binding by CaBP. Prog Clin Biol Res. 1988; 252:115–120. [PubMed: 3347614]
41. Spencer R, Charman M, Wilson PW, Lawson DEM. The relationship between vitamin D-stimulated calcium transport and intestinal calcium-binding protein in the chicken. Biochem J. 1978; 170:93–101. [PubMed: 204303]
42. Krisinger J, Strom M, Darwish HD, Perlman K, Smith C, DeLuca HF. Induction of calbindin-D 9k mRNA but not calcium transport in rat intestine by 1,25-dihydroxyvitamin D3 24-homologs. J Biol Chem. 1991; 266:1910–3. [PubMed: 1988453]
43. Akhter S, Kutuzova GD, Christakos S, DeLuca HF. Calbindin D9k is not required for 1,25-dihydroxyvitamin D3-mediated Ca2+ absorption in small intestine. Arch Biochem Biophys. 2007; 460:227–232. [PubMed: 17224126]
44. Kutuzova GD, Akhter S, Christakos S, Vanhooke J, Kimmel-Jehan C, DeLuca HF. Calbindin D(9k) knockout mice are indistinguishable from wild-type mice in phenotype and serum calcium level. Proc Natl Acad Sci U S A. 2006; 103:12377–12381. [PubMed: 16895982]
45. Mattson MP, Rychlik B, Chu C, Christakos S. Evidence for calcium-reducing and excito-protective roles for the calcium-binding protein calbindin-D28k in cultured hippocampal neurons. Neuron. 1991; 6:41–51. [PubMed: 1670921]
46. Chard PS, Bleakman D, Christakos S, Fullmer CS, Miller RJ. Calcium buffering properties of calbindin D28k and parvalbumin in rat sensory neurones. J Physiol. 1993; 472:341–357. [PubMed: 8145149]

47. Liu Y, Porta A, Peng X, Gengaro K, Cunningham EB, Li H, Dominguez LA, Bellido T, Christakos S. Prevention of glucocorticoid-induced apoptosis in osteocytes and osteoblasts by calbindin-D28k. J Bone Miner Res. 2004; 19:479–490. [PubMed: 15040837]
48. Dowd DR, MacDonald PN, Komm BS, Haussler MR, Miesfeld RL. Stable Expression of the Calbindin-D28K Complementary-Dna Interferes with the Apoptotic Pathway in Lymphocytes. Molecular Endocrinology. 1992; 6:1843–1848. [PubMed: 1336124]
49. Schroder B, Schlumbohm C, Kaune R, Breves G. Role of calbindin-D_{9k} in buffering cytosolc free Ca^{2+} ions in pig duodenal enterocytes. J Physiol. 1996; 492:715–722. [PubMed: 8734984]
50. Lambers TT, Mahieu F, Oancea E, Hoofd L, de LF, Mensenkamp AR, Voets T, Nilius B, Clapham DE, Hoenderop JG, Bindels RJ. Calbindin-D28K dynamically controls TRPV5-mediated Ca2+ transport. EMBO J. 2006; 25:2978–2988. [PubMed: 16763551]
51. Kerry DM, Dwivedi PP, Hahn CN, Morris HA, Omdahl JL, May BK. Transcriptional synergism between vitamin D-responsive elements in the rat 25-hydroxyvitamin D3 24-hydroxylase (CYP24) promoter. J Biol Chem. 1996; 271:29715–29721. [PubMed: 8939905]
52. Christakos S, Barletta F, Huening M, Dhawan P, Liu Y, Porta A, Peng X. Vitamin D target proteins: Function and regulation. Journal of Cellular Biochemistry. 2003; 88:238–244. [PubMed: 12520521]
53. Anderson PH, O'Loughlin PD, May BK, Morris HA. Quantification of mRNA for the vitamin D metabolizing enzymes CYP27B1 and CYP24 and vitamin D receptor in kidney using real-time reverse transcriptase- polymerase chain reaction. J Mol Endocrinol. 2003; 31:123–132. [PubMed: 12914530]
54. Favus MJ, Langman CB. Evidence for calcium-dependent control of 1,25-dihydroxyvitamin D3 production by rat kidney proximal tubules. J Biol Chem. 1986; 261:11224–11229. [PubMed: 2426268]
55. Berghard A, Gradin K, Toftgard R. Serum and extracellular calcium modulate induction of cytochrome P-450IA1 in human keratinocytes. J Biol Chem. 1990; 265:21086–21090. [PubMed: 1979076]
56. Baran DT, Milne ML. 1,25 Dihydroxyvitamin D increases hepatocyte cytosolic calcium levels. A potential regulator of vitamin D-25-hydroxylase. J Clin Invest. 1986; 77:1622–1626. [PubMed: 3084563]
57. Bronner F, Buckley M. The molecular nature of 1,25-(OH)2-D3-induced calcium-binding protein biosynthesis in the rat. Adv Exp Med Biol. 1982; 151:355–360. [PubMed: 6897481]
58. Darwish HM, DeLuca HF. Identification of a 1,25-dihydroxyvitamin D3-response element in the 5'-flanking region of the rat calbindin D-9k gene. Proc Natl Acad Sci USA. 1992; 89:603–607. [PubMed: 1309950]
59. Jeung EB, Leung PC, Krisinger J. The human calbindin-D9k gene. Complete structure and implications on steroid hormone regulation. J Mol Biol. 1994; 235:1231–1238. [PubMed: 8308886]
60. Colnot S, Romagnolo B, Lambert M, Cluzeaud F, Porteu A, Vandewalle A, Thomasset M, Kahn A, Perret C. Intestinal expression of the calbindin-D9K gene in transgenic mice. Requirement for a Cdx2-binding site in a distal activator region. J Biol Chem. 1998; 273:31939–31946. [PubMed: 9822664]
61. Colnot S, Ovejero C, Romagnolo B, Porteu A, Lacourte P, Thomasset M, Perret C. Transgenic analysis of the response of the rat calbindin-D 9k gene to vitamin D. Endocrinology. 2000; 141:2301–2308. [PubMed: 10875229]
62. Wang L, Klopot A, Freund JN, Dowling LN, Krasinski SD, Fleet JC. Control of Differentiation-Induced Calbindin-D_{9k} Gene Expression in Caco-2 Cells by Cdx-2 adn HNF-1α . Am J Physiol. 2004; 287:G943–G953.
63. Duflos C, Bellaton C, Pansu D, Bronner F. Calcium solubility, intestinal sojourn time and paracellular permeability codetermine passive calcium absorption in rats. J Nutr. 1995; 125:2348–2355. [PubMed: 7666252]

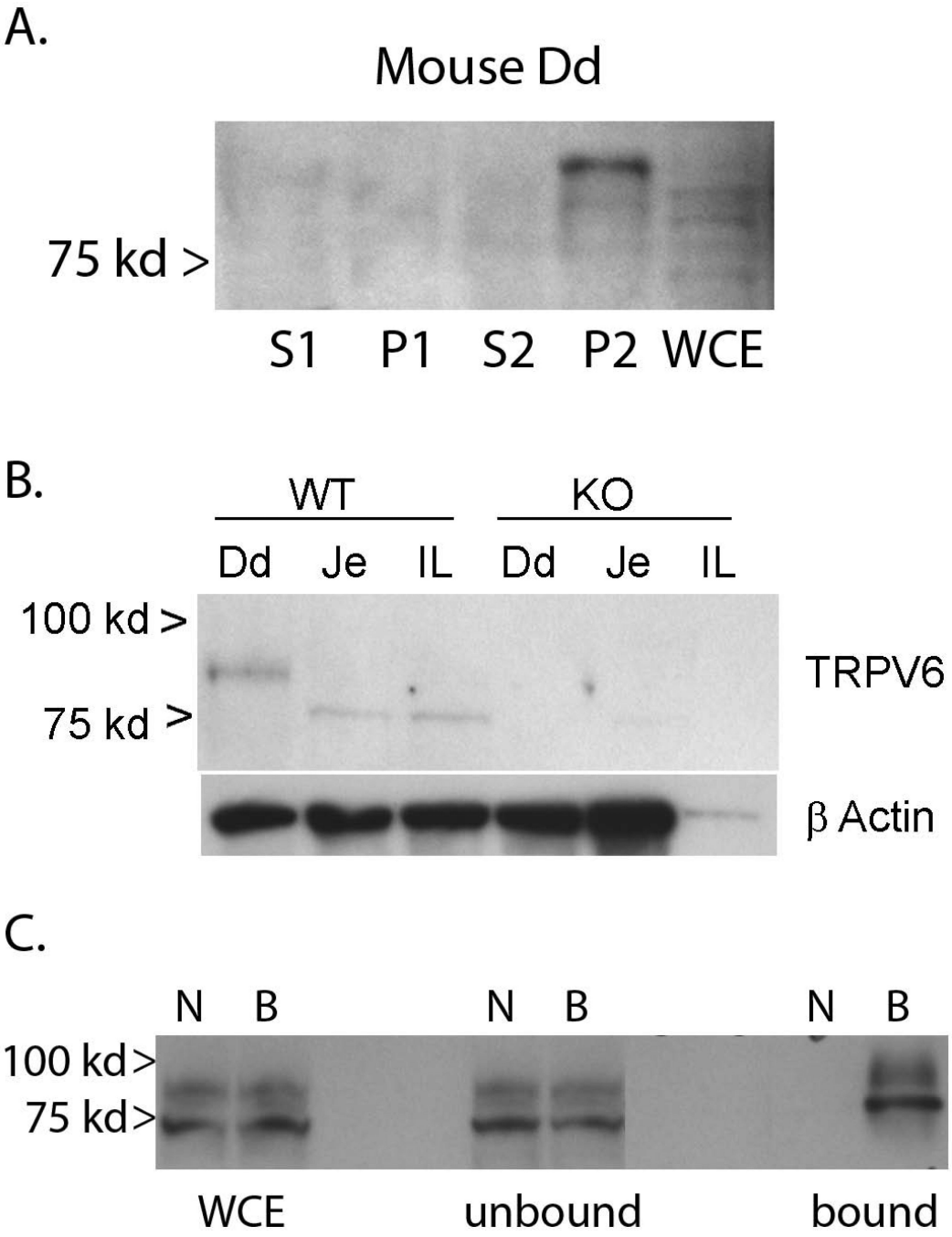

Figure 1. Expression of TRPV6 in mouse intestine and in transiently transfected Caco-2 cells

(A) Cell fractions from the duodenum of 8-week-old C57BL/6J mice were prepared and analyzed for TRPV6 protein levels by Western blot analysis. S1, P1 = supernatant and pellet from the initial centrifugation; S2, P2 = supernatant and pellet resulting from centrifugation of a resuspended P1 pellet. P2 contains brush border membranes. WCE = whole cell extracts (WCE). (B) Brush border membrane fractions from the duodenum (Dd), jejunum (Je), and Ileum (IL) of eight week old wild-type (WT) and VDR knockout (KO) mice were analyzed by Western blot analysis for TRPV6 and β actin (loading control). (C) hTRPV6 protein levels and membrane location in 50% confluent cultures of Caco-2 cells transiently transfected with the pN3XFlag-hTRPV6. Two days after transfection cell surface proteins

were labeled by biotinylation and biotin-labeled proteins were isolated using an Avidin-bound agarose column. Whole cell extracts (WCE), flow-through from the column (unbound), and material bound to the column (bound) from non-labeled cells (N) and biotin-labeled cells (B) were examined for 3XFlag-tagged hTRPV6 by Western blot analysis.

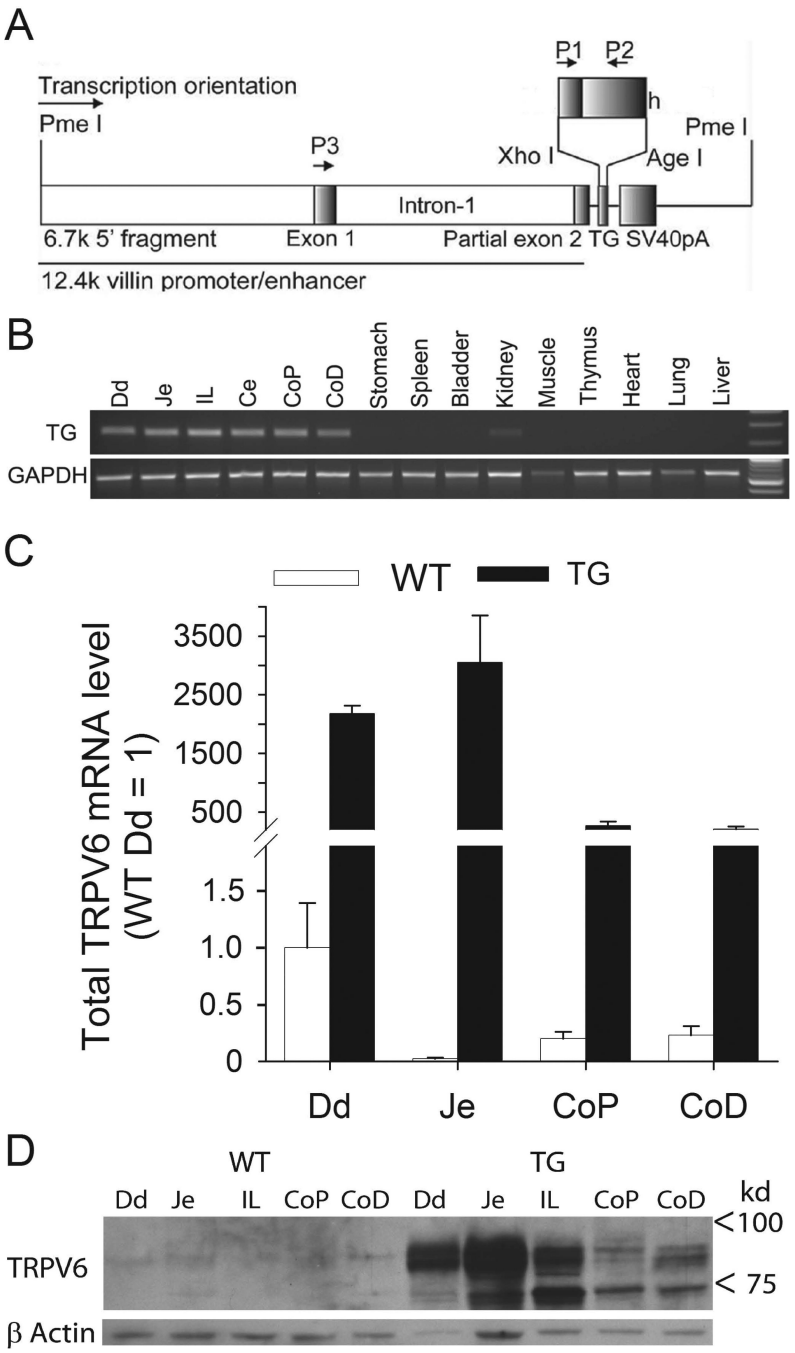

Figure 2. Generation of intestine-specific, flag-tagged human TRPV6 expressing transgenic mice

(A) Transgene construct. A 12.4 kb villin promoter/enhancer was used to drive expression of a 3XFlag-tagged-human TRPV6 cDNA transgene in the intestine epithelial cells. Primers P1 and P2 were used for genotyping; primers P3 and P2 were used for assessing transgene mRNA levels. (B) PCR analysis of transgene mRNA expression in mouse tissues (Dd, duodenum; Je, jejunum; IL, ileum; CoP, proximal colon; CoD, distal colon). (C) Total TRPV6 mRNA levels (mouse and transgenic) in the intestinal segments of wild type and transgenic mice (TG) was determined by real-time PCR as described in methods. Bars represent mean ± SEM, n=4. (D) TRPV6 and β-actin protein levels were determined by

Western blot analysis of whole cell extracts from mucosal scrapings from different segments of wild type (WT) and transgenic mice (TG).

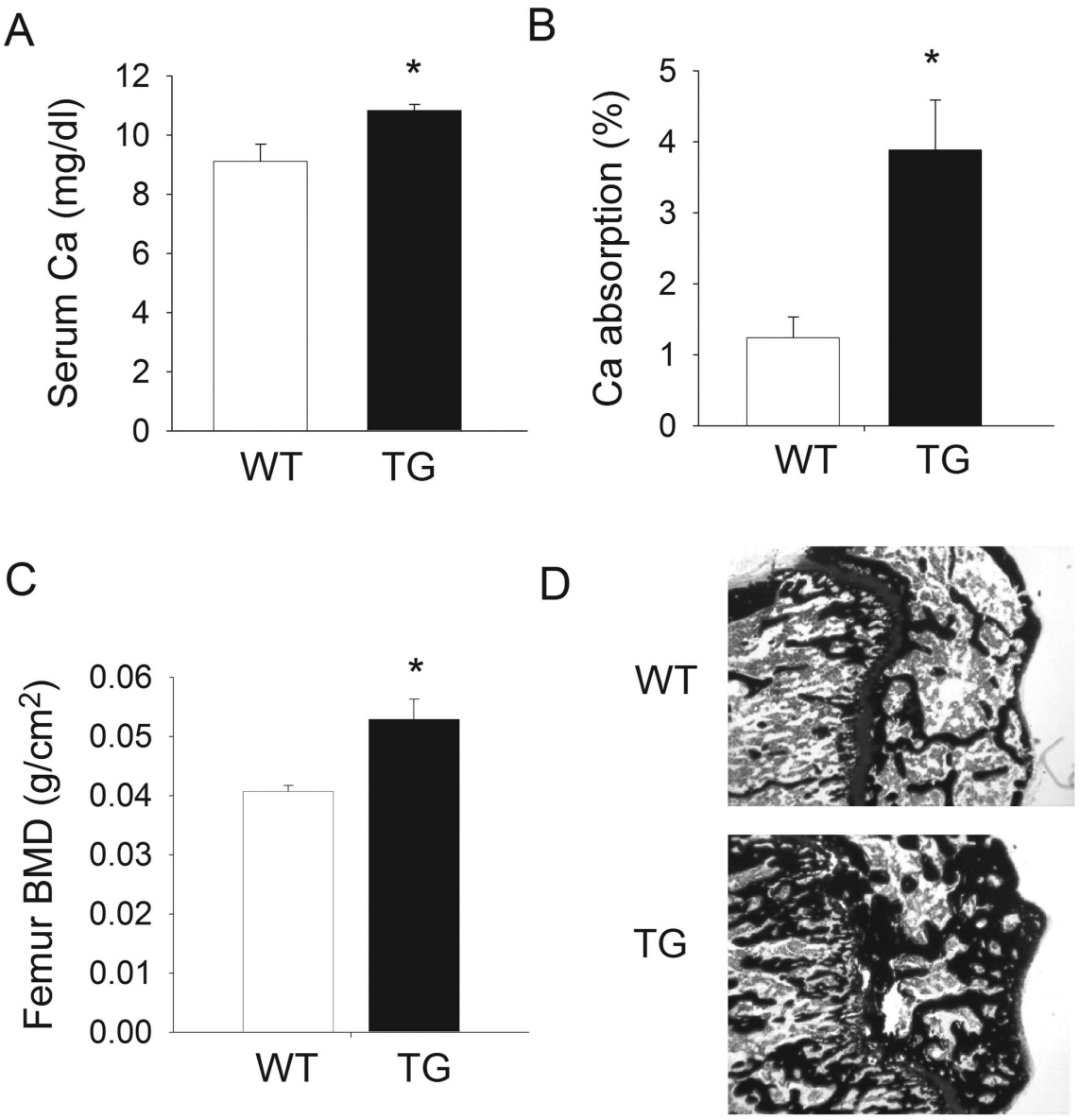

Figure 3. Calcium (Ca) absorption, serum Ca, and skeletal phenotypes in wild type (WT) and TRPV6 transgenic (TG) mice

8-wk-old WT and TG mice were fed a 0.25% Ca diet from weaning. (A) Serum Ca. (B) Duodenal Ca absorption. (C) Femoral bone mineral density (BMD) was determined using dual energy x-ray absorption (DEXA). In panels A-C, Bars represent mean ± SEM, n=8-9 (Ca absorption) or n=4 (serum Ca, bone phenotypes), *p<0.05 compared to WT. (D) Representative micrographs of calcified, plastic-embedded, von Kossa stained sections from the distal femur. (magnification 4X).

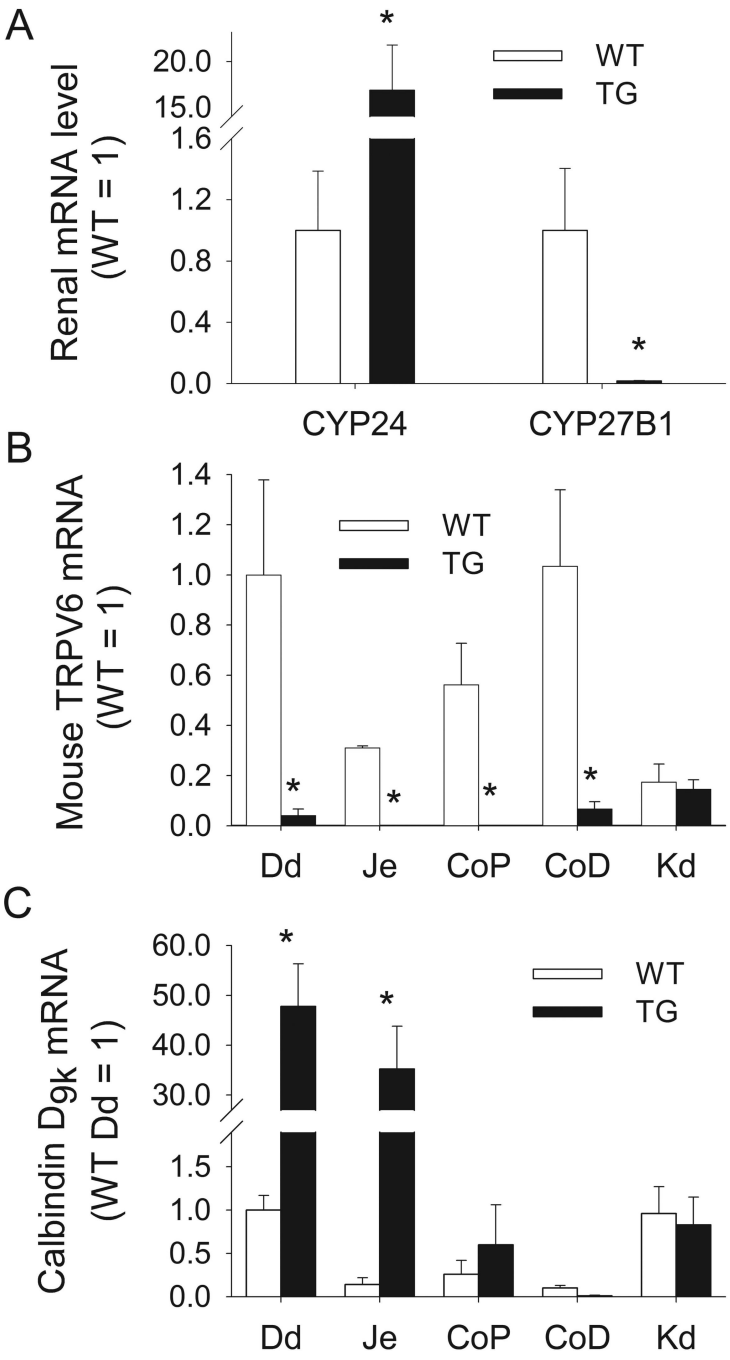

Figure 4. Renal and intestinal gene expression in wild type (WT) and TRPV6 transgenic mice (TG)

8-wk-old female WT and TG mice were fed a 0.25% Ca diet from weaning. (A) Renal CYP24 and CYP27B1 mRNA. (B) Mouse TRPV6 mRNA expression in intestine segments. (C) Calbindin D_{9k} mRNA expression in intestine segments. Bars represent mean ± SEM, n=4-5, *p<0.05 compared to WT.

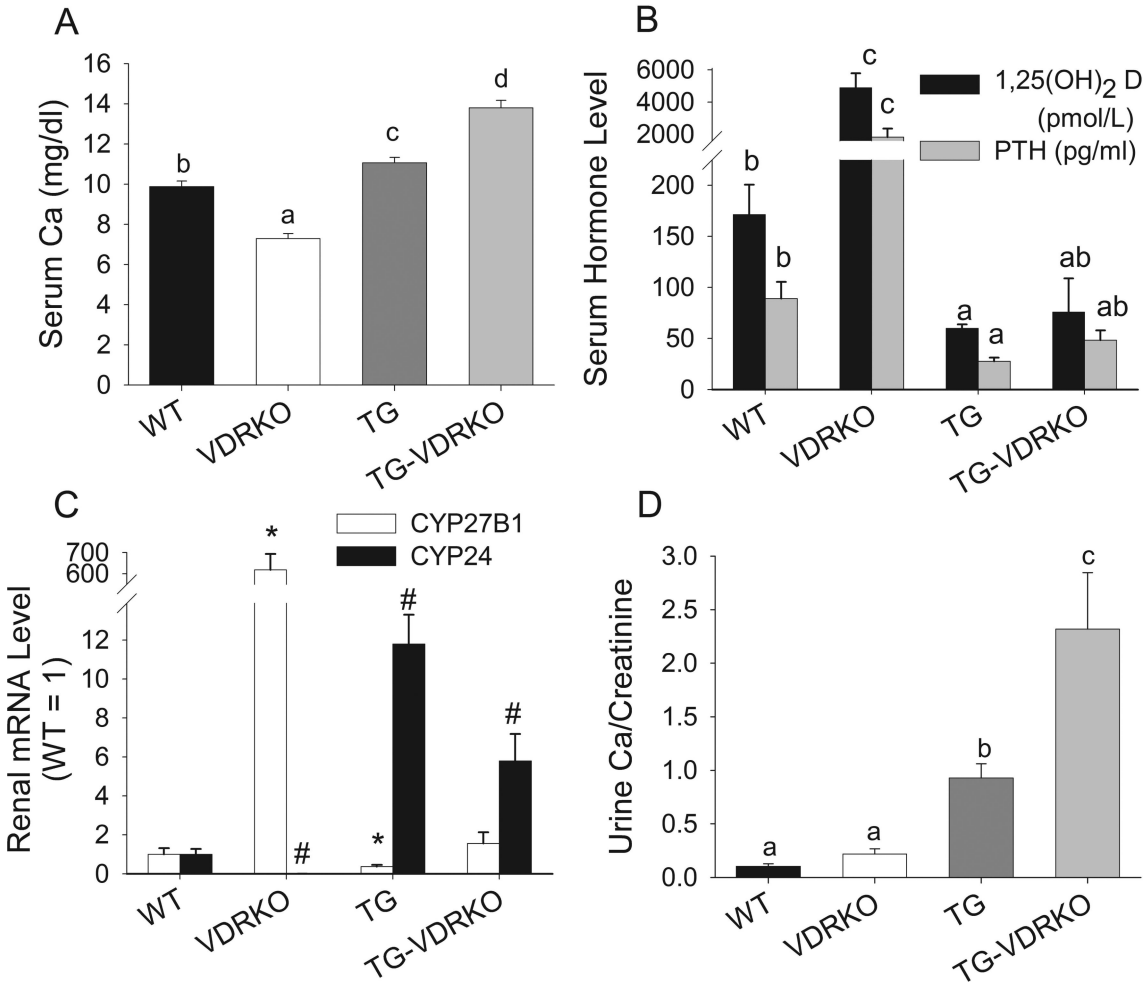

Figure 5. Serum Ca, 1,25(OH)$_2$ D, and PTH, renal gene expression, and urine Ca in wild type (WT), VDR knockout (VDRKO), TRPV6 transgenic (TG), and transgene-recovered (TG-VDRKO) mice

Mice were fed diets with 0.5% Ca from weaning to 10-wks of age. (A) Serum Ca (n=4/group) (B) Serum 1,25(OH)$_2$ D and PTH (n=5-12/group). (C) Renal CYP27B1 and CYP24 mRNA (n=4/group). (D) Urine Ca/creatinine ratio (n=4/group) Bars represent mean ± SEM. In panels A, B, D groups without a common letter superscript differ significantly, $p<0.05$. In panel C, * different from all other bars for CYP27B1, $p < 0.05$; # different from all other bars for CYP24, $p < 0.05$.

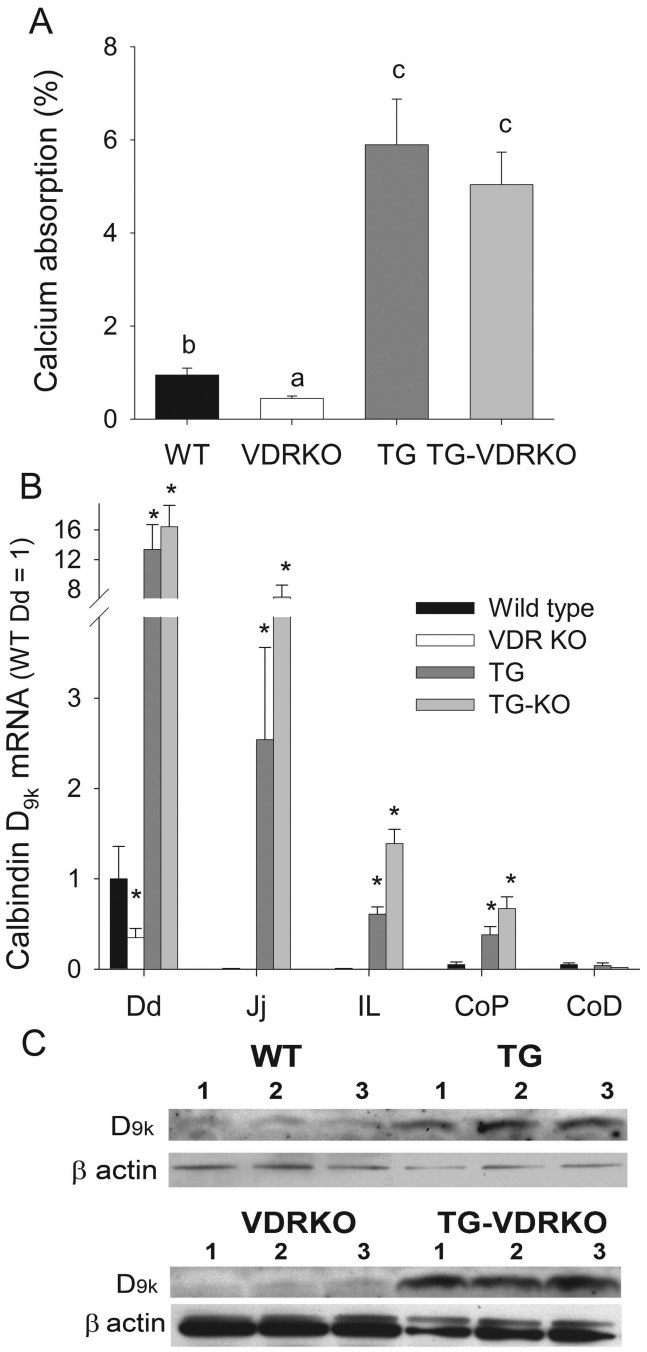

Figure 6. Calcium (Ca) absorption and intestinal calbindin D_{9k} expression in wild type (WT), VDR knockout (VDRKO), TRPV6 transgenic (TG), and transgene-recovered (TG-VDRKO) mice

Mice were fed diets with 0.5% Ca from weaning to 10-wks of age. (A) Duodenal Ca absorption. (n=6-10/group). (B) Calbindin D_{9k} mRNA expression in duodenum (Dd), jejunum (Jj), ileum (IL) proximal colon (CoP) and distal colon (CoD) (n=4-7/group). In panels A and B, bars represent mean ± SEM. In panel A, groups without a common letter superscript differ significantly, $p<0.05$. In panel B, * $p < 0.05$ vs WT within a tissue. (C) Calbindin D_{9k} protein expression in duodenum (n=3 per group).

Table 1

μCT analysis of distal femora from 8 wk old wild type (WT) and TRPV6 transgenic (TG) mice fed a 0.25% Ca diet from weaning.

	WT (n=5)	TG (n=3)
Trabecular bone (distal femur)		
BV/TV (%)	2.7±0.6	24.5±1.5*
Tb.N (1/mm)	3.78±0.16	6.74±0.21*
Tb.Th (mm)	0.026±0.001	0.043±0.002*
Tb.Sp (mm)	0.266±0.012	0.137±0.005*
Cortical bone		
Ct.Ar/Tt.Ar (%)	37.2±0.8	45.7±0.4*
Ct. Th (mm)	0.143±0.002	0.180±0.005*

Ct.Ar/Tt.Ar = cortical area fraction; Ct.Th = cortical thickness; BV/TV = ratio of trabecular bone volume to total volume in the distal femur; Tb.N = trabecular number, Tb.Th = trabecular thickness Tb.Sp = trabecular spacing

* $p < 0.05$

Table 2

μCT analysis of femora from 10 wk old wild type (WT), VDR knockout (VDRKO), TRPV6 transgenic (TG), and transgene recovered VDR knockout (TG-VDRKO) mice fed a 0.5% Ca diet from weaning.

	WT	VDRKO	TG	TG-VDRKO
Femur length (mm)	15.05±0.08^{b}	12.20±0.19^{a}	15.04±0.04^{b}	14.48±0.43^{b}
Trabecular bone (distal femur)				
BV/TV (%)	9.1±1.4^{b}	0.5±0.1^{a}	27.8±1.5^{c}	33.9±3.7^{c}
Tb.N (1/mm)	4.89±0.16^{b}	1.97±0.123^{a}	8.45±0.30^{c}	9.35±1.09^{c}
Tb.Th (mm)	0.036±0.002^{b}	0.026±0.001^{a}	0.040±0.001^{bc}	0.044±0.001^{c}
Tb.Sp (mm)	0.201±0.007^{b}	0.531±0.037^{c}	0.111±0.004^{a}	0.103±0.014^{a}
Cortical bone				
Ct.Ar/Tt.Ar (%)	43.7±0.9^{b}	28.9±1.6^{a}	52.9±1.8^{c}	48.4±2.1^{bc}
Ct.Th (mm)	0.180±0.009^{b}	0.076±0.005^{a}	0.240±0.011^{c}	0.214±0.012^{c}

Values are means ± SEM (n=4). Within a phenotype, values without a common letter superscript differ significantly, $p<0.05$ (Fisher's protected LSD).

Ct.Ar/Tt.Ar = cortical area fraction; Ct.Th = cortical thickness; BV/TV = ratio of trabecular bone volume to total volume in the distal femur; Tb.N = trabecular number, Tb.Th = trabecular thickness Tb.Sp = trabecular spacing